

Sensor Placement for Learning in Flow Networks

Arnav Burudgunte*

Arlei Silva*

Abstract

Large infrastructure networks (e.g. for transportation and power distribution) require constant monitoring for failures, congestion, and other adversarial events. However, assigning a sensor to every link in the network is often infeasible due to placement and maintenance costs. Instead, sensors can be placed only on a few key links, and machine learning algorithms can be leveraged for the inference of missing measurements (e.g. traffic counts, power flows) across the network. This paper investigates the sensor placement problem for networks. We first formalize the problem under a flow conservation assumption and show that it is NP-hard to place a fixed set of sensors optimally. Next, we propose an efficient and adaptive greedy heuristic for sensor placement that scales to large networks. Our experiments, using datasets from real-world application domains, show that the proposed approach enables more accurate inference than existing alternatives from the literature. We demonstrate that considering even imperfect or incomplete ground-truth estimates can vastly improve the prediction error, especially when a small number of sensors is available.

Keywords: Networks, graphs, sensor placement, semi-supervised learning, active learning.

1 Introduction

This paper addresses the problem of effectively placing sensors to estimate edge flows in networks. Given a flow value at each edge, our goal is to choose a set of edges to monitor in order to infer values at unmonitored edges. Versions of our problem appear in infrastructure networks, such as traffic [15], water [19], and power [25] networks. We assume that each edge in the network has some associated value (e.g. traffic flow, water flow, electrical current) that must be measured to track congestion, anomalies, and other events. Owing to the size of the network and measurement cost, we often cannot place a sensor at every edge. A common solution is to place sensors at a small subset of the edges and estimate the rest using semi-supervised learning [31, 15, 37]. Because the choice of this subset can seriously alter the prediction quality, our goal is to efficiently select a subset that yields the most accurate estimate.

We focus here on values obeying the assumption *flow conservation*, meaning the sum of flows into a vertex is (approximately) equal to the sum of flows out of it.

The sensor placement problem is related to two machine learning paradigms. The first is *semi-supervised learning (SSL)*, in which models learn from both labeled and unlabeled data. SSL is motivated by applications where the availability of labeled data is limited [29, 35]. Graph-based SSL is useful when a dataset can be encoded as a graph with labels on nodes or edges; the unlabeled data can be leveraged by propagating labels through the graph structure.

The second machine learning paradigm related to sensor placement is *active learning*, in which a model iteratively makes requests for specific observations to be labeled [26, 8, 7]. When applied to graph data, active learning can take advantage of the graph structure to select samples to be labeled more effectively [2, 4, 12]. Such algorithms often assume no prior information about the ground-truth labels at first and slowly learn more about the network as more data is labeled. In practice, however, we often have outside information about the edge labels before placing any sensors. For example, urban planners have detailed predictions for traffic flow based on traffic demand models, spatial and temporal data, and other factors [1, 22, 20]. Such estimates can be extremely useful for inferring labels with a small number of sensors because they significantly constrain the possible solutions—there might be many possible predictions that satisfy the flow conservation assumption, but only a few will correctly predict the volume of traffic at major roads. As we will show, even an imperfect estimate of edge values can generate a more effective choice of sensors than a naive algorithm that makes predictions based on flow conservation alone.

The question we address in this paper is *how to select a small number of edge flows to be monitored such that the error of flow predictions for the remaining of the network is minimized*. As the problem is NP-hard, we propose an efficient algorithm that greedily selects sensors to minimize the error of a flow conservation-based prediction, combining knowledge of the network topology and ground-truth flow values. However, the efficiency of our algorithm depends on the efficient evaluation of possible sensor locations. We achieve

*Rice University, {ab141,arlei}@rice.edu

this objective via two optimizations, the lazy evaluation of candidate sensors and the fast evaluation of the benefit of adding each sensor using the Woodbury matrix identity. Our experiments evaluate the proposed algorithm in terms of accuracy and running time and show that it outperforms several alternatives.

We summarize our main contributions as follows:

- We provide a formal statement of the sensor placement problem under flow conservation, with proof that the problem is NP-complete;
- We propose an efficient greedy heuristic for sensor placement that combines two optimizations to speed up the computation of each greedy decision;
- We compare the proposed heuristic against several alternatives using real networks and the experimental results show that our approach is more accurate while the proposed optimizations lead to significant savings in computing time.

2 Related Work

Graph-Based Semi-Supervised Learning

Graph-based SSL is a special case of SSL where observations can be encoded as vertices and edges represent relations between them [37]. Label propagation [35, 36] is the most popular technique for reconstructing smooth values. More recently, flow-based SSL [15] was proposed to infer conserved flows on the edges rather than smooth vertex labels. However, the conservation-based solution can be highly dependent on the choice of labeled edges and the nature of the data [35, 15, 10], which is a motivation for our work. We focus on the problem of selecting edges to be labeled (or sensor locations, in the case of infrastructure networks), which is a special case of the active learning problem [26].

Active Learning on Graphs With the exception of [15], active learning on graphs has been studied exclusively on the vertices under a smoothness assumption. Cut-based methods [13], error bound minimization [12], and sampling (signal processing) [11] methods have been proposed as active learning strategies. In all these algorithms, the choice of nodes or edges is made using only the network topology, and thus cannot be optimized using the ground-truth values [13, 15]. Such methods apply the eigenvectors of the Laplacian matrix as a basis for vertex signals to sample vertices as to enforce smoothness. Conversely, the corresponding basis for edge flows—the singular vectors of the incidence matrix—has many vectors with frequency 0, making it difficult to prioritize samples. We thus assume that edges are chosen by optimizing a reconstruction loss. We show that this approach allows us to match the per-

formance of existing baselines using far fewer sensors.

Traffic Forecasting The problem of forecasting traffic flows, speeds, and other attributes is can be motivated by smart city applications. Early attempts at traffic prediction infer network flows from a set of origin-destination pairs [1] or vice versa [14]; the popular traffic simulator SUMO [22] operates using a similar principle. More recently, deep learning has been used to predict traffic as a function of spatial and temporal data [20, 24, 27]. The relevant result for our work is that there are sophisticated, accurate models available for predicting traffic flow in graphs even without labels from sensors. We show that even when such estimates are noisy or imperfect, they provide useful information about ground-truth flows. We focus on the spatial dimension of the problem and use simpler inference models such as label propagation, but our algorithms could be generalized to use any forecasting model.

Sensor Placement and Influence Maximization Previous work has studied sensor placement for other objectives such as monitoring spatial phenomena [17] and detecting contaminants in water distribution networks [18, 19]. Similar to these problems, we study sensor placement as a combinatorial optimization problem, though we minimize a prediction error rather than a fixed penalty function. Closely related to sensor placement is the influence maximization problem, which asks for the best subset of nodes to target for influence such that after some diffusion process, the maximum number of nodes have been influenced [16]. Solutions often depend on the diffusion model, which predicts the number of nodes affected by the chosen seed set [21]. Instead of using a process, we apply a machine learning model to make predictions based on a validation set (i.e. set of edge observations). Moreover, we notice that, although we apply similar greedy algorithms as those previously used for sensor placement and influence maximization, our objective functions are not submodular [23].

3 Problem Definition

3.1 Preliminaries We represent a network as an unweighted graph $G = (V, E)$ with a set V of n vertices and set E of m edges. The graph is represented by the adjacency matrix $\mathbf{A} \in \mathbb{R}^{n \times n}$, where $\mathbf{A}_{ij} = 1$ if an edge exists between vertices i and j and $\mathbf{A}_{ij} = 0$ otherwise.

We are interested in the value given by vector $\mathbf{f} \in \mathbb{R}^m$ where \mathbf{f}_i is the flow at edge i . We represent the values of a subset $E' \subset E$ as a vector $\mathbf{x}_{E'} \in \mathbb{R}^{|E'|}$. Thus a set of labeled (sensor) edges S is represented by the corresponding value $\mathbf{f}_S \in \mathbb{R}^{|S|}$, and a set of unlabeled (target) edges T is represented as $\mathbf{f}_T \in \mathbb{R}^{|T|}$.

3.2 General Sensor Placement Problem The sensor placement problem can be divided into two parts. The first part predicts the values of unlabeled edges based on a given set of sensors. The second is choosing a set of sensors that yields the prediction with the lowest error. We formalize both parts here.

3.2.1 Prediction Given a labeled set of k sensors S and corresponding observed flows $\mathbf{f}_S \in \mathbb{R}^k$, we produce an estimate $\hat{\mathbf{f}}$ for \mathbf{f} via graph-based semi-supervised learning. The divergence on each vertex i is defined as the difference between flows out of i and flows into i :

$$(3.1) \quad \text{div}(i) = \sum_{e \in E: e \text{ out of } i} \mathbf{f}_e - \sum_{e \in E: e \text{ into } i} \mathbf{f}_e$$

Flows for missing edges are estimated by minimizing the sum of squared divergences given by

$$(3.2) \quad \|\mathbf{B}\mathbf{f}\|^2 = \sum_{i \in V} (\text{div}(i))^2$$

where the incidence matrix $\mathbf{B} \in \mathbb{R}^{n \times m}$ is defined as

$$(3.3) \quad \mathbf{B}_{ij} = \begin{cases} 1 & \text{if edge } e_j \text{ enters node } i \\ -1 & \text{if edge } e_j \text{ leaves node } i \\ 0 & \text{otherwise.} \end{cases}$$

For undirected graphs, we first choose an arbitrary orientation for each edge before constructing \mathbf{B} . We then minimize the sum of the divergence and a regularization term parameterized by $\lambda \in \mathbb{R}_+$:

$$(3.4) \quad \begin{aligned} \hat{\mathbf{f}}^* &= \arg \min_{\hat{\mathbf{f}} \in \mathbb{R}^m} \|\mathbf{B}\hat{\mathbf{f}}\|^2 + \lambda^2 \cdot \|\hat{\mathbf{f}}\|^2 \\ \text{s.t. } \hat{\mathbf{f}}_S &= \mathbf{f}_S \end{aligned}$$

where λ guarantees that the solution is unique.

The resulting optimization problem can be rewritten as a regularized least squares. Define $\mathbf{f}_S^0 \in \mathbb{R}^m$ such that $\mathbf{f}_i^0 = \mathbf{f}_i$ if $i \in S$ and $\mathbf{f}_i^0 = 0$ otherwise. Let $\mathbf{H}_T \in \mathbb{R}^{m \times (m-k)}$ be a matrix (map) such that $\mathbf{H}_{ij} = 1$ if flow \mathbf{f}_i maps to $(\mathbf{f}_T)_j$ (i.e., they correspond to the same edge). The least-squares formulation is [6, 10]:

$$(3.5) \quad \mathbf{f}_T^* = \arg \min_{\mathbf{f}_T \in \mathbb{R}^{m-k}} \|\mathbf{B}\mathbf{H}_T\mathbf{f}_T - \mathbf{B}\mathbf{f}_S^0\|^2 + \lambda^2 \cdot \|\mathbf{f}_T\|^2$$

3.2.2 Sensor Placement Given a set T of target vertices, a set C of candidate vertices, and budget k , our problem is to choose the subset of k vertices in C that yields the best prediction for T :

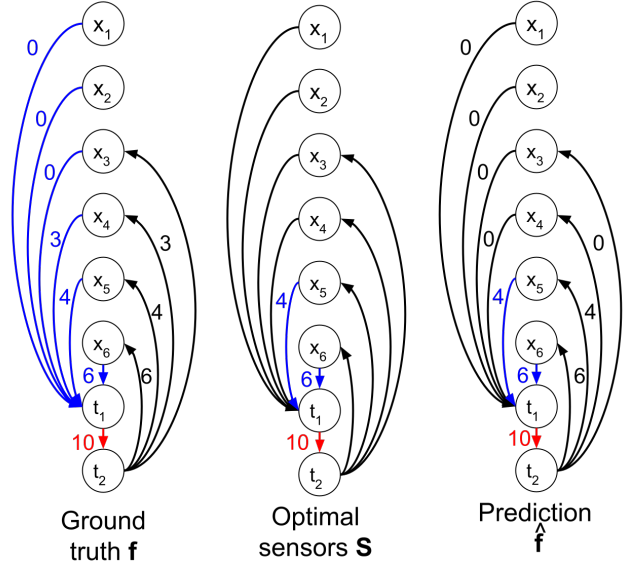


Figure 1: Reducing *SUM* to *SENSOR*, with $X = \{3, 4, 6\}$ and $t = 10$, candidate set $C = X$ (blue), and the target $T = \{(t_1, t_2)\}$ (red). Choosing the two edges that sum to t for S generates a perfect prediction for T .

$$(3.6) \quad \begin{aligned} S^* &= \arg \min_{S \subseteq C, |S|=k} \|\hat{\mathbf{f}}_T - \mathbf{f}_T\|^2 \\ \text{s.t. } \hat{\mathbf{f}}_T &= \phi(\mathbf{f}_S, S, \lambda) \end{aligned}$$

where ϕ is the prediction model (see Section 3.2.1).

3.3 Hardness We now formally define the sensor placement problem and show that it is NP-complete.

DEFINITION 1. (THE SENSOR PLACEMENT PROBLEM) Given a graph G , a candidate set of edges $C \subseteq E$, a target set of edges $T \subseteq E$, a budget k , and an error ϵ , $\text{SENSOR}(G, C, T, k)$ consists of determining whether there exists a set of edge labels $S \subseteq C$ such that $|S| = k$ and the edge predictions $\hat{\mathbf{f}}$ for S (see Equation 3.6) have an error $\|\hat{\mathbf{f}}_T - \mathbf{f}_T\| \leq \epsilon$.

THEOREM 3.1. *Sensor Placement is NP-complete.*

Proof. Given a certificate $S \subseteq C$ of edges selected as sensors, we can clearly compute $\hat{\mathbf{f}}$ and check the error in polynomial time. Let $\text{SUM}(X, t)$ be an instance of the subset sum problem for a finite set $X \subseteq \mathbb{Z}_+$ and $t \in \mathbb{Z}_+$. The problem is to find a subset $X' \subset X$ such that $\sum_{x \in X'} x = t$. This problem is NP-hard [9].

We can reduce an arbitrary instance of *SUM* to *SENSOR* by constructing graph G as follows. Create a

vertex for each element in X and two additional vertices t_1 and t_2 . Add a set of edges $C = \{(x, t_1) : x \in X\}$, each with a flow equal to s ; an edge (t_1, t_2) with flow t ; and set of edges $\{(t_2, x) : x \in X\}$ each with flow x . Finally, add $|X|$ vertices with 0 flow into t_1 .

There exists a solution to $SENSOR(G, C, \{(t_1, t_2)\}, k)$ with prediction error $\epsilon = 0$ iff one exists for $SUM(X, t)$. The equivalence is straightforward: if some set X' sums to t , choose edges $\{(x', t_1) : x' \in X'\}$, whose flows also sum to t , as sensors. If $|X'| < k$, choose edges with 0 flow for the remaining sensors. Since there is only edge out of t_1 , that edge must have flow t . Conversely, if k sensors correctly predict the flow on (t_1, t_2) , their flows must sum to t , and thus provide a solution to SUM . \square

3.4 Submodularity The submodularity property [23] is often applied to provide approximation guarantees for poly-time algorithms that solve sensor placement and other NP-hard related problems on graphs [16, 19]. However, it is straightforward to show that our sensor placement objective is not submodular. This is because the objective from Equation 3.6 is not monotonically decreasing. The addition of a new sensor might increase the error of the flow predictions. For example, consider a triangle where only one edge e has a nonzero flow. With no sensors, Equation 3.5 predicts $\hat{\mathbf{f}} = 0$, resulting in an error of $|\mathbf{f}_e|^2$. After choosing e as a sensor, the prediction becomes \mathbf{f}_e everywhere, and the error increases to $2|\mathbf{f}_e|^2$. One could consider a simplified version of our problem as a maximum flow coverage problem, where the goal is to place the sensors as to maximize the total flow covered by the sensors. This simplified version of the problem is submodular.

4 Methods

4.1 Greedy Heuristic Given our hardness result (Theorem 3.1), we propose a greedy algorithm that iteratively selects the sensor that minimizes the prediction error in Equation 3.6. The pseudocode is given in Algorithm 1. At each of the k iterations (lines 2-11), the algorithm selects the best new sensor s^* based on its resulting prediction error ϵ (lines 6-10).

The flow prediction problem is not submodular (see Section 3.4). In practice, however, it is almost always possible to add a sensor that decreases the prediction error, and thus the problem exhibits (empirical) diminishing return (see Figure 2). This property enables our algorithm to work well in practice.

At each of the k iterations, our algorithm evaluates the benefit of every not yet chosen edge in C . This requires $O(m)$ solutions of the least-squares problem in Equation 3.5. Each instance takes $O(m^3)$ time to

Algorithm 1 Sensor Placement(G, C, T, k, \mathbf{f})

```

1:  $S \leftarrow \emptyset$ 
2: for  $i = 1, \dots, k$  do
3:    $\epsilon_{min} \leftarrow \infty$ 
4:   for all  $s \in C - S$  do
5:      $S' = S \cup \{s\}$ 
6:      $\epsilon = \|\phi(\mathbf{f}_{S'}, S', \lambda) - \mathbf{f}_T\|_2^2$ 
7:     if  $\epsilon < \epsilon_{min}$  then
8:        $\epsilon_{min} \leftarrow \epsilon$ 
9:        $s^* = s$ 
10:    end if
11:  end for
12:   $S \leftarrow S \cup \{s^*\}$ 
13: end for
return  $S$ 

```

solve, giving an overall running time of $O(m^5)$. We now propose two strategies to speed up this algorithm.

4.2 Lazy Evaluation Previous works have proposed lazy evaluation to speed up greedy algorithms for submodular optimization [19]. As discussed in Section 3.4, our sensor placement problem is not submodular but the associated coverage problem—maximizing the total flow coverage—is submodular. Based on this “near-submodularity” property, we propose applying lazy evaluation to speed up Algorithm 1. More specifically, we will assume that (1) adding a sensor does not increase the flow prediction error and (2) the benefit of adding a sensor at a later iteration does not increase its benefit (i.e. its flow prediction error reduction).

The lazy evaluation works as follows. Before choosing any sensors, we compute the benefit of each edge and store the results in a heap. At each iteration, we recompute the benefit of the best remaining edge. If it remains the best, then it is highly unlikely any other edge can overtake it, and we can choose that edge without reevaluating any other benefits. This saves up to $|C|$ evaluations per iteration. In case the evaluation decreases the rank of the top edge, we evaluate the next edge returned by the heap until the rank is unchanged.

4.3 Recursive Computation We also propose a recursive computation to speed up the predictions themselves after a new labeled edge is revealed. The goal is to avoid solving Equation 4.3 from scratch after a single new sensor is introduced. Instead, we will re-use results from previous iterations to quickly update flow predictions as new sensors are selected.

Our approach is similar to the recurrence for vertex labels given in [34] but works edge flows. To simplify the notation, let $\mathbf{X}_T = \mathbf{B}\mathbf{H}_T$. Then we can rewrite the

closed form solution to Equation 3.5 as

$$\hat{\mathbf{f}}_T = -(\mathbf{X}_T^T \mathbf{X}_T + \lambda^2 \mathbf{I})^{-1} \mathbf{X}_T^T \mathbf{B} \mathbf{f}_S^0$$

which requires a matrix inversion.

We first compute an LU-decomposition of $\mathbf{X}_T^T \mathbf{X}_T + \lambda^2 \mathbf{I}$ and use it to solve for $\hat{\mathbf{f}}_T$. Now suppose we select edge $e_i = e_{T_j}$, updating $S' \leftarrow S \cup \{e_i\}$ and $T' \leftarrow T - \{e_i\}$. The update is equivalent to removing the j th column of \mathbf{X}_T or removing the j th row and column of $\mathbf{X}_T^T \mathbf{X}_T$. This is a rank two update and can be written in terms of matrices $\mathbf{U}, \mathbf{V} \in \mathbb{R}^{t \times 2}$ ($t = |T|$) defined as

$$\mathbf{U} = \begin{pmatrix} -1 & 0 \\ 0 & (\mathbf{X}_T^T \mathbf{X}_T)_{j,1} \\ \vdots & \vdots \\ 0 & (\mathbf{X}_T^T \mathbf{X}_T)_{j,t} \end{pmatrix}, \mathbf{V} = \begin{pmatrix} 0 & -1 \\ (\mathbf{X}_T^T \mathbf{X}_T)_{1,j} & 0 \\ \vdots & \vdots \\ (\mathbf{X}_T^T \mathbf{X}_T)_{t,j} & 0 \end{pmatrix}$$

Further, let us define the downsampling matrix $\mathbf{S}_j \in \mathbb{R}^{(t-1) \times t}$ such that $\mathbf{S}_j \mathbf{X}_T$ removes the j th row of \mathbf{X}_T . It follows that

$$(\mathbf{X}_{T'}^T \mathbf{X}_{T'})^{-1} = \mathbf{S}_j (\mathbf{X}_T^T \mathbf{X}_T + \mathbf{U} \mathbf{V}^T)^{-1} \mathbf{S}_j^T$$

We now use the previously-computed LU-decomposition to solve for $\mathbf{Y} = (\mathbf{X}_{T'}^T \mathbf{X}_{T'} + \lambda^2 \mathbf{I})^{-1} \mathbf{U}$ and $\mathbf{z} = (\mathbf{X}_{T'}^T \mathbf{X}_{T'} + \lambda^2 \mathbf{I})^{-1} \mathbf{S}_j^T \mathbf{X}_{T'}^T \mathbf{B} \mathbf{f}_{S'}^0$. Finally, we apply the Woodbury identity [33] as follows:

$$\begin{aligned} \hat{\mathbf{f}}_{T'} &= -(\mathbf{X}_{T'}^T \mathbf{X}_{T'} + \lambda^2 \mathbf{I})^{-1} \mathbf{X}_{T'}^T \mathbf{B} \mathbf{f}_{S'}^0 \\ &= -\mathbf{S}_j (\mathbf{X}_T^T \mathbf{X}_T + \lambda^2 \mathbf{I} + \mathbf{U} \mathbf{V}^T)^{-1} \mathbf{S}_j^T \mathbf{X}_{T'}^T \mathbf{B} \mathbf{f}_{S'}^0 \\ &= -\mathbf{S}_j (\mathbf{z} - \mathbf{Y} (\mathbf{I} + \mathbf{V}^T \mathbf{Y})^{-1} \mathbf{V}^T \mathbf{z}) \end{aligned}$$

As a result, the only matrix that must be inverted directly is $\mathbf{I} + \mathbf{V}^T \mathbf{Y}$, but since this is a 2×2 matrix the inversion can be done in constant time. The LU-decomposition of $\mathbf{X}_T^T \mathbf{X}_T$, which is performed $O(m)$ times, has time complexity $O(m^3)$ [3]. Solving a linear system using the decomposition takes $O(m^2)$ time, giving a new overall complexity of $O(m^4)$.

5 Experimental Results

We test our proposed algorithm on real-world traffic networks. We consider two settings. First, we assume that our method is able to fully observe flow values to place the sensors, which is the ideal scenario. Next, we consider a more realistic setting where flows are unknown or only partially known.

5.1 Experimental Settings

5.1.1 Datasets We use traffic flows on road networks from Anaheim, Barcelona, Chicago, and Winnipeg (see

Table 1: Road Networks Used for Experiments

Network	n	m
Anaheim	416	914
Barcelona	1020	2522
Chicago	933	2950
Winnipeg	1052	2836

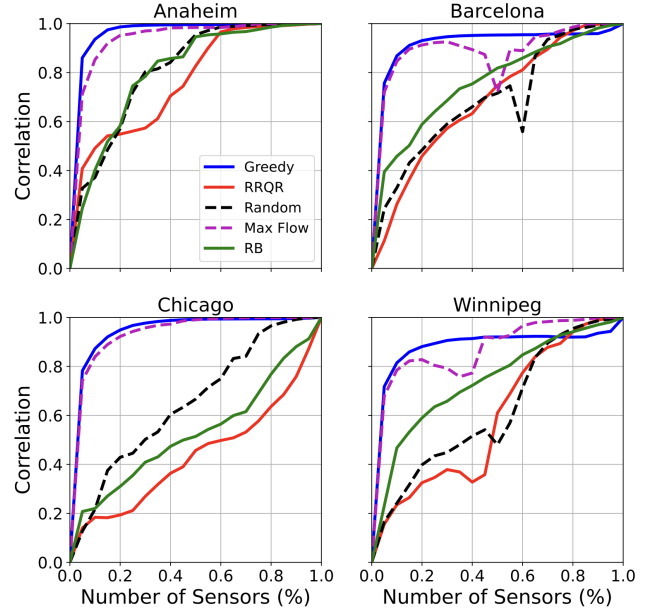


Figure 2: Conserved flow prediction results when flows are fully observed for validation purposes. The plots show the correlation between the prediction $\hat{\mathbf{f}}$ and ground truth flow \mathbf{f} . Our greedy heuristic (Greedy) outperforms all four baselines in all datasets.

Table 1) [28]. The nodes in each network represent intersections and edges represent roads between them. Each network is represented as a directed graph where the direction of an edge corresponds to the direction of traffic flow. The flows are generated

5.1.2 Hyperparameters We set $\lambda = 10^{-6}$ when solving the least-squares formulation for flow prediction.

5.1.3 Baselines We compare our flow selection method with four baselines. First, random selection (Random) simply chooses the next edge uniformly at random from the currently unchosen edges. Second, recursive bisection (RB) [15] partitions the graph using spectral clustering and chooses edges crossing the new cut as the next sensors. The idea is to find "bottleneck"

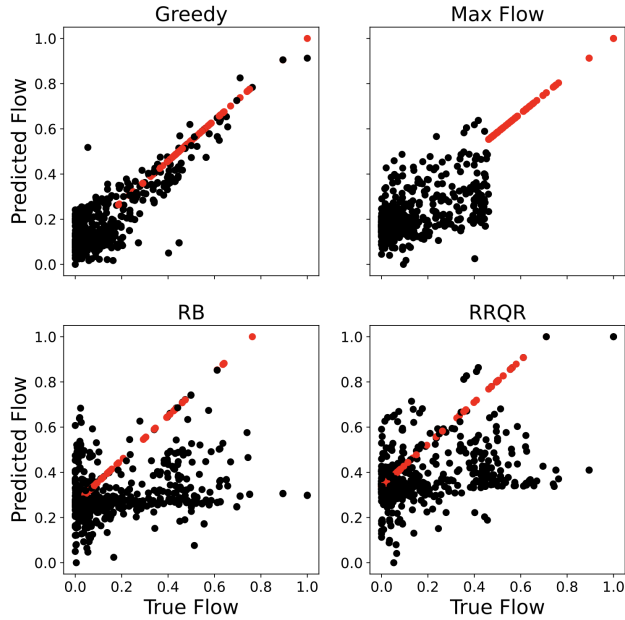


Figure 3: Predicted vs. ground-truth flows for the Anaheim road network using the flow conservation algorithm (Equation 3.5) for various sensor placement algorithms. Values for the selected sensors are shown in red and inferred values in black. The budget k is fixed at 10% of all edges. Both the predicted and actual flows are normalized to $[0,1]$. Our method (Greedy) chooses a more representative set of edges than the baselines.

edges where major flows are concentrated, such as highways. Recursive bisection has been found to work well when much of the flow is not conserved [15]. Third, rank-revealing QR (RRQR) [5] exploits a known bound on the error of the flow conservation algorithm. If the SVD of the incidence matrix $\mathbf{B} \in \mathbb{R}^{n \times m}$ is given by $\mathbf{B} = \mathbf{U}\mathbf{\Sigma}\mathbf{V}^T$, then the $m - n + 1$ rightmost columns \mathbf{V}_C of \mathbf{V} give a basis for the cycle space of fully conserved flows. The $n - 1$ leftmost columns \mathbf{V}_R give a basis for the cut space of flows with nonzero divergence. If S is a set of $m - n + 1$ linearly independent rows of \mathbf{V}_C corresponding to the selected sensors, then the reconstruction error is bounded by

$$(5.7) \quad \|\hat{\mathbf{f}} - \mathbf{f}\| \leq (\sigma_{\min}^{-1}(\mathbf{V}_{SC}) + 1) \cdot \|\mathbf{V}_R \mathbf{f}\|$$

RRQR uses a greedy heuristic to minimize this bound by minimizing $\sigma_{\min}^{-1}(\mathbf{V}_{SC})$ [15].

Finally, maximum flow (Max Flow) selects the k edges with the highest flows:

$$S^* = \arg \max_{S \subseteq E} \|\mathbf{f}_S\|$$

where \mathbf{f}_S is the vector of flows for edges in S .

5.1.4 Evaluation Metrics:

Correlation (Corr):

$$Corr = \frac{cov(\hat{\mathbf{f}}, \mathbf{f})}{\sigma(\hat{\mathbf{f}}) \cdot \sigma(\mathbf{f})}$$

where cov and σ are the covariance and std, respectively.

Mean squared error (MSE):

$$MSE = \frac{1}{m} \|\mathbf{f} - \hat{\mathbf{f}}\|^2$$

Mean absolute error (MAE):

$$MAE = \frac{1}{m} \sum_{e \in E} |\mathbf{f}_e - \hat{\mathbf{f}}_e|$$

Mean absolute percentage error (MAPE):

$$MAPE = \frac{1}{m} \sum_{e \in E} \left| \frac{\mathbf{f}_e - \hat{\mathbf{f}}_e}{\mathbf{f}_e} \right|$$

Max error (MAX):

$$MAX = \max_{e \in E} |\mathbf{f}_e - \hat{\mathbf{f}}_e|$$

5.2 Fully-Observed Flows

We assume access to the ground truth flows \mathbf{f} while choosing the sensors.

Figure 2 shows the correlation between predicted and ground-truth flows for a varying number of sensors (as a percentage). Our approach significantly outperforms the flow-agnostic baselines, especially when the number of sensors is small (20% or less). The results also show that there is no clear best baseline among the flow-agnostic methods. In most cases, our algorithm also outperforms Max Flow. The greedy algorithm has the additional advantage of being monotone; that is, adding a sensor greedily almost always improves the prediction. This is not always the case for Max Flow.

Table 2 shows the prediction errors in terms of all the evaluation metrics for a fixed budget of 10% of the candidate sensors being selected. Our greedy solution consistently outperforms the baselines according to most metrics (Corr, MSE, and MAE) and is often competitive with the baselines in terms of MAPE and MAX. We notice that the objective applied by our algorithm is quite different from MAPE (skewed towards small flows) and MAX (skewed towards large flows).

To distinguish our greedy algorithm and Max Flow, Figure 3 shows the predicted vs ground-truth flows for the Anaheim dataset. The results show the superiority of our approach, especially for intermediate value flows.

5.3 Synthetic and Noisy Flows

In this section, we remove the assumption that flows are fully observed.

Table 2: Flow prediction error in terms of Correlation Coefficient (Corr), Mean Squared Error (MSE), Mean Absolute Error (MAE), Mean Absolute Percentage Error (MAPE), and Maximum Error (MAX). Our approach (Greedy) consistently outperforms the baselines on all metrics except for MAPE.

		Corr (\uparrow)	MSE (\downarrow)	MAE (\downarrow)	MAPE(\downarrow)	MAX (\downarrow)
Anaheim	Greedy	0.936	0.006	0.051	194.381	0.452
	Max Flow	0.852	0.014	0.076	264.498	0.577
	RB	0.402	0.043	0.130	209.277	0.963
	RRQR	0.493	0.038	0.121	246.388	0.818
	Random	0.491	0.039	0.128	241.370	0.998
Barcelona	Greedy	0.869	0.008	0.062	289.385	0.450
	Max Flow	0.847	0.009	0.066	283.837	0.393
	RB	0.458	0.024	0.096	275.972	0.884
	RRQR	0.264	0.024	0.101	181.948	0.901
	Random	0.303	0.029	0.099	157.793	1.010
Chicago	Greedy	0.873	0.007	0.059	102.544	0.323
	Max Flow	0.840	0.009	0.067	111.540	0.319
	RB	0.220	0.023	0.096	103.362	0.992
	RRQR	0.184	0.024	0.099	95.762	1.000
	Random	0.259	0.022	0.094	92.863	0.994
Winnipeg	Greedy	0.815	0.013	0.081	217.534	0.561
	Max Flow	0.785	0.015	0.087	213.350	0.591
	RB	0.467	0.031	0.110	133.450	0.931
	RRQR	0.235	0.036	0.118	116.715	0.961
	Random	0.270	0.035	0.113	113.394	0.986

5.3.1 Synthetic Flows We generate synthetic flows under the conservation assumption (see the appendix [15]). The greedy heuristic is computed using the prediction error on the synthetic flows, and the resulting sensors are tested on the true flows for the four traffic networks. The sensor placements based on synthetic flows do not always outperform the baselines (see Figure 5). This is evidence that the synthetic flows are not an effective proxy for the real flows.

5.3.2 Noisy Estimates Now we consider the setting where our model has access to noisy estimates of the ground-truth flows (e.g. based on the macro traffic demand model for a city [30, 32]). For each edge e_i , we simulate a noisy estimate $\mathbf{f}_i + \epsilon$ with noise $\epsilon \sim N(0, r\sigma)$ where σ is the standard deviation of \mathbf{f} and $r \in \mathbb{R}$ controls the amount of noise. Figure 5 shows the correlation between the predicted and original ground-truth flows for varying noise levels. The results show that our approach (Noisy Greedy) is robust to noise and often outperforms the baselines. As expected, Max Flow is also robust to noise—as ϵ is not relative to edge flow values, the noise has little effect on large flows.

5.3.3 Visualization Figure 4 shows the sensors placed by our heuristic and the Recursive Bisection (RB) baseline (flow agnostic) for the Anaheim network. We notice that our approach identifies high-traffic paths while also minimizing redundancy.

5.4 Speedups To evaluate the optimizations proposed in Sections 4.2 and 4.3, we run Algorithm 1 using a brute force evaluation of the heuristic, with lazy evaluation, and with a combination of lazy evaluation and recursive computation. The brute force evaluation takes over an hour to choose 10% of the edges in most of the networks tested, but lazy evaluation with recursive computation reduces the running time to a few seconds. Figure 6 shows the speedups.

6 Conclusion and Ongoing Work

We have proposed an approach for sensor placement for semi-supervised learning in flow networks that accounts for ground-truth values. We show that choosing the optimal set of sensors is NP-hard and provides an effective greedy heuristic for the problem. We also provide two optimizations to further speed-up the proposed heuristic. Our experiments show that our meth-

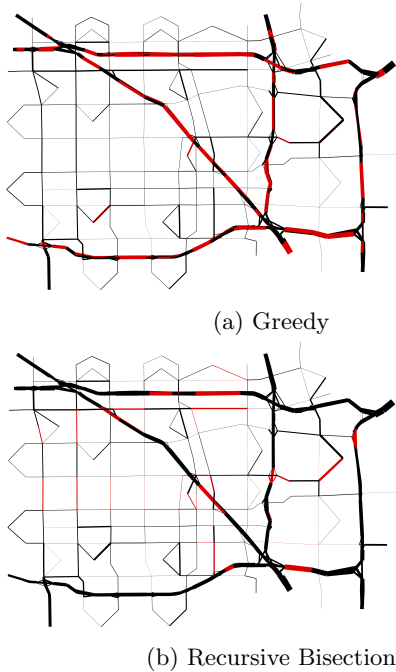


Figure 4: Example of sensor placements (in red) using our heuristic (Greedy) and the Recursive Bisection (RB) baseline for the Anaheim road network. Edge traffic counts are represented by edge thickness. Unlike the baseline, our approach targets a few high-traffic paths.

ods significantly outperform baselines that account only for the graph topology and that the proposed optimizations lead to significant running time savings.

Our work opens several venues for future investigation. We are particularly interested in even faster flow-aware sensor placement algorithms based on matrix factorization. This requires the discovery of effective bases for the sparse representation of flows. In terms of applications, we will study how the proposed solutions can be applied to wastewater monitoring.

7 Acknowledgements

This research was partially funded by the 100K Strong IFCE-Rice-SENAI Program on AI for Urban Sustainability and Resilience to Natural Disasters in the Americas, the US Department of Transportation (USDOT) Tier-1 University Transportation Center (UTC) Transportation Cybersecurity Center for Advanced Research and Education (CYBER-CARE), and the Rice Office of Undergraduate Research and Inquiry.

References

[1] Hillel Bar-Gera. Origin-based algorithm for the

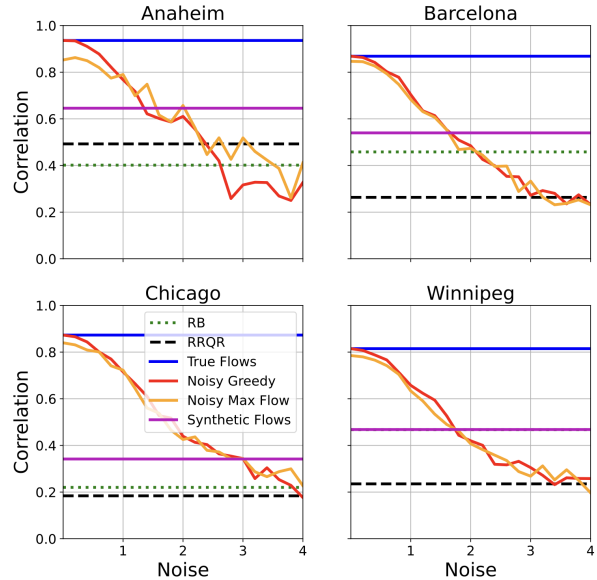


Figure 5: Conserved flow prediction results for sensor selection based on a noisy estimate of ground-truth flows for varying noise levels. The number of sensors placed (k) is fixed at 10% of the edges. The sensor placement is quite robust to noise target values, outperforming the baselines under noise levels of up to $2\times$ the standard deviation of the flows.

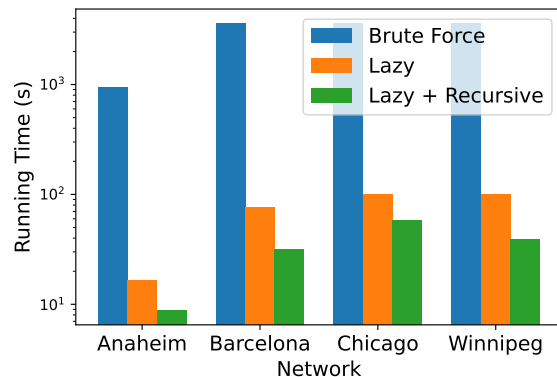


Figure 6: Running time of Algorithm 1 using brute force, lazy evaluation without and with recursive computation for four networks. The number of sensors k is set to 10% of all edges. In all cases, combining lazy evaluation with the recursive evaluation provided significant speedups. The brute force solution was truncated at 1 hour for all networks except Anaheim.

traffic assignment problem. *Transportation Science*, 36(4):398–417, 2002.

[2] Mustafa Bilgic, Lilyana Mihalkova, and Lise Getoor.

- Active learning for networked data. In *ICML*, 2010.
- [3] James R. Bunch and John E. Hopcroft. Triangular factorization and inversion by fast matrix multiplication. *Mathematics of Computation*, 28(125):231–236, 1974.
 - [4] N Cesa Bianchi, Claudio Gentile, F Vitale, and G Zappella. Active learning on trees and graphs. In *COLT*, 2010.
 - [5] Tony F. Chan. Rank revealing qr factorizations. *Linear Algebra and its Applications*, 88-89:67–82, 1987.
 - [6] Donghui Chen and Robert J Plemmons. Nonnegativity constraints in numerical analysis. *The Birth Of Numerical Analysis*, pages 109–139, 2010.
 - [7] David Cohn, Les Atlas, and Richard Ladner. Improving generalization with active learning. *Machine learning*, 15:201–221, 1994.
 - [8] David A Cohn, Zoubin Ghahramani, and Michael I Jordan. Active learning with statistical models. *JMLR*, 4:129–145, 1996.
 - [9] Thomas H. Cormen, Charles E. Leiserson, Ronald L. Rivest, and Clifford Stein. *Introduction to Algorithms, Third Edition*. The MIT Press, 3rd edition, 2009.
 - [10] Arlei Lopes da Silva, Furkan Kocayusufoglu, Saber Jafarpour, Francesco Bullo, Ananthram Swami, and Ambuj Singh. Combining physics and machine learning for network flow estimation. In *ICLR*, 2020.
 - [11] Akshay Gadde, Aamir Anis, and Antonio Ortega. Active semi-supervised learning using sampling theory for graph signals. In *SIGKDD*, 2014.
 - [12] Quanquan Gu and Jiawei Han. Towards active learning on graphs: An error bound minimization approach. In *ICDM*, 2012.
 - [13] Andrew Guillory and Jeff A Bilmes. Label selection on graphs. In *NeurIPS*, 2009.
 - [14] Martin L Hazelton. Inference for origin–destination matrices: estimation, prediction and reconstruction. *Transportation Research Part B: Methodological*, 35(7):667–676, 2001.
 - [15] Junteng Jia, Michael T. Schaub, Santiago Segarra, and Austin R. Benson. Graph-based semi-supervised & active learning for edge flows. In *SIGKDD*, 2019.
 - [16] David Kempe, Jon Kleinberg, and Éva Tardos. Maximizing the spread of influence through a social network. In *SIGKDD*, 2003.
 - [17] Andreas Krause, Carlos Guestrin, Anupam Gupta, and Jon Kleinberg. Near-optimal sensor placements: Maximizing information while minimizing communication cost. In *IPSN*, 2006.
 - [18] Andreas Krause, Jure Leskovec, Carlos Guestrin, Jeanne VanBriesen, and Christos Faloutsos. Efficient sensor placement optimization for securing large water distribution networks. *Journal of Water Resources Planning and Management*, 134(6):516–526, 2008.
 - [19] Jure Leskovec, Andreas Krause, Carlos Guestrin, Christos Faloutsos, Jeanne VanBriesen, and Natalie Glance. Cost-effective outbreak detection in networks. In *SIGKDD*, 2007.
 - [20] Mengzhang Li and Zhanxing Zhu. Spatial-temporal fusion graph neural networks for traffic flow forecasting. In *AAAI*, 2021.
 - [21] Yuchen Li, Ju Fan, Yanhao Wang, and Kian-Lee Tan. Influence maximization on social graphs: A survey. *IEEE TKDE*, 30(10):1852–1872, 2018.
 - [22] Pablo Alvarez Lopez, Michael Behrisch, Laura Bieker-Walz, Jakob Erdmann, Yun-Pang Flötteröd, Robert Hilbrich, Leonhard Lüken, Johannes Rummel, Peter Wagner, and Evamarie Wießner. Microscopic traffic simulation using sumo. In *ITSC*, 2018.
 - [23] George L Nemhauser, Laurence A Wolsey, and Marshall L Fisher. An analysis of approximations for maximizing submodular set functions–I. *Mathematical programming*, 14:265–294, 1978.
 - [24] Hao Peng, Hongfei Wang, Bowen Du, Md Zakirul Alam Bhuiyan, Hongyuan Ma, Jianwei Liu, Lihong Wang, Zeyu Yang, Linfeng Du, Senzhang Wang, et al. Spatial temporal incidence dynamic graph neural networks for traffic flow forecasting. *Information Sciences*, 521:277–290, 2020.
 - [25] Ananth Narayan Samudrala, M. Hadi Amini, Soumya Kar, and Rick S. Blum. Optimal sensor placement for topology identification in smart power grids. In *CISS*, 2019.
 - [26] Burr Settles. Active learning literature survey. 2009.
 - [27] Chao Song, Youfang Lin, Shengnan Guo, and Huaiyu Wan. Spatial-temporal synchronous graph convolutional networks: A new framework for spatial-temporal network data forecasting. In *AAAI*, 2020.
 - [28] Ben Stabler, Hillel Bar-Gera, and Elizabeth Sall. Transp. networks for research. <https://github.com/bstabler/TransportationNetworks>, 2016.
 - [29] Amarnag Subramanya and Partha Pratim Talukdar. *Graph-Based Semi-Supervised Learning*. Morgan & Claypool Publishers, 2014.
 - [30] OZ Tamin and LG Willumsen. Transport demand model estimation from traffic counts. *Transportation*, 16:3–26, 1989.
 - [31] Yuichi Tanaka, Yonina C. Eldar, Antonio Ortega, and Gene Cheung. Sampling signals on graphs: From theory to applications. *IEEE Signal Processing Magazine*, 37(6):14–30, 2020.
 - [32] Luis G Willumsen. Simplified transport models based on traffic counts. *Transportation*, 10(3):257–278, 1981.
 - [33] Max A. Woodbury. Inverting modified matrices. In *Memorandum Rept. 42, Statistical Research Group*, page 4. Princeton University, 1950.
 - [34] Xiaojin Zhu. *Semi-Supervised Learning with Graphs*. PhD thesis, Carnegie Mellon University, 2005.
 - [35] Xiaojin Zhu and Zoubin Ghahramani. Learning from labeled and unlabeled data with label propagation. Technical report, School of Computer Science, CMU, 2003.
 - [36] Xiaojin Zhu, Zoubin Ghahramani, and John Lafferty. Semi-supervised learning using gaussian fields and harmonic functions. In *ICML*, 2003.
 - [37] Xiaojin Zhu, Jaz Kandola, John Lafferty, and Zoubin Ghahramani. Graph Kernels by Spectral Transforms. In *Semi-Supervised Learning*. MIT Press, 09 2006.